

Electron-transfer reactions studied by laser-induced optoacoustics: Learning about chromophore-medium (protein) interactions*

Silvia E. Braslavsky

Max-Planck-Institut für Strahlenchemie, Postfach 10 13 65, D-45413 Mülheim an der Ruhr, Germany

Abstract: The ability of time-resolving enthalpy (ΔH) and structural volume (ΔV) changes in the nano- to μs time range offered by laser-induced optoacoustic spectroscopy (LIOAS) opens the possibility of a stepwise thermodynamic analysis of chromophore-medium interactions upon photoinduced reactions in biological systems. We applied LIOAS to biological photoreceptors, as well as to model systems, with the purpose of understanding the origin of ΔV in electron-transfer (ET) reactions in those systems. The linear correlation between the counterion-dependent volume changes and ΔH for the free-radical formation upon ET quenching of erythrosin dianion triplet, ${}^3\text{Er}^{2-}$, by $\text{Mo}(\text{CN})_8^{4-}$ and of $\text{Ru}(\text{bpy})_3^{2+}$ by MV^{2+} is interpreted in terms of an enthalpy–entropy compensation owing to the strong influence of the counterions on the water hydrogen-bond network in which the reactants are embedded. The relatively large entropic term determined for radical formation thus originates in water rearrangements during the process. The increasing contraction in acetonitrile, propionitrile, butyronitrile, and valeronitrile for the ET quenching of ${}^3\text{Zn}$ -tetraphenylporphyrin by 1,4-benzoquinone is understood by considering the increasing interaction strength between the electron-pair donor nitriles and ZnTPP^+ . Thus, in polar environments, specific chromophore-medium (solvent or proteins) interactions, in addition to electrostriction, should be considered to explain the time-resolved ΔV and ΔH values.

INTRODUCTION

Biological photoreceptors may be divided according to their function into four groups: (i) the antenna pigments that very quickly transfer the energy of the light of various wavelengths to the reaction centers; (ii) the energy converters that transform the light energy into chemical energy, and in which the primary photochemical process is either an electron transfer, as is the case in the chlorophyll-protein complexes in the various photosystems in plants and bacteria, or a double-bond isomerization, as is the case in bacteriorhodopsin [1] and most certainly in the recently discovered proteorhodopsin [2]; (iii) the sensory pigments that sense the quality and quantity of light around the organism (vide infra for details); and (iv) the DNA repair enzyme photolyases in which a blue-light absorbing chromophore acting as an antenna transfers the energy to a two-electron reduced flavin-adenin dinucleotide (FADH^-), which in turn transfers an electron to the dimerized nucleotides (dimerized as a result of UV damage) for repair [3].

The covalently linked chromophore in several of the photosensors undergoes a double-bond isomerization as the primary photochemical step. That is the case for retinal in rhodopsin [4,5] and sen-

*Lecture presented at the XIXth IUPAC Symposium on Photochemistry, Budapest, Hungary, 14–19 July 2002. Other presentations are published in this issue, pp. 999–1090.

sory rhodopsins [6], of open-chain tetrapyrrols in phytochromes of plants [7], bacteria [8], and cyanobacteria [9], as well as of *p*-hydroxycinnamic anion in photoactive yellow protein [10]. In the recently identified sensory photoreceptors such as phototropin, however, the photoinduced reaction is a reaction of the noncovalently linked flavin triplet with a nearby cysteine residue in the protein [11].

A common feature of energy converters and sensory pigments is that upon excitation they all give rise to a series of intermediates with lifetimes ranging from femtoseconds to seconds that reflect rapid excited-state deactivation, the primary photochemical event, plus protein movements as well as chromophore conformational changes in the cases of flexible chromophores (e.g., retinals, *p*-hydroxycinnamic anion, and open-chain tetrapyrrols). After excited-state deactivation and the primary photochemical event, all subsequent reactions in chromoproteins are thermal reactions taking place on the ground-state potential energy surface and therefore not well suited for fluorescence studies. In most cases, the intermediates have strongly overlapping absorption spectra both with each other and with the parent state. This impairs quantitative determinations of, for example, quantum yields, by optical methods.

Photocalorimetry, laser-induced optoacoustic spectroscopy

In view of the above-mentioned features, phototransformations of biological photoreceptors were studied already decades ago by means of a photocalorimetric technique. W. W. Parson's group [12] noticed that the pressure signal upon pulsed excitation consists of two components, one due to volume changes produced by the heat evolved upon radiationless deactivation and the other due to structural rearrangements in the molecule and its surroundings. In aqueous media, it was possible to separate both contributions by varying the temperature between the value at which the expansion coefficient $\beta = 0$ (3.9 °C for neat water) and room temperature, in view of the strong variation of β in these media.

Laser-induced optoacoustic spectroscopy (LIOAS, Fig. 1) is a sensitive photothermal technique permitting the study of the time evolution of heat and volume changes. Lasers with pulse widths of a few nanoseconds have improved the time resolution to the limit imposed by the slow acoustic waves. Thus, in the parallel arrangement between excitation beam direction and detector, the transit time of the generated acoustic wave across the laser cross-section determines the time resolution of ca. 15 ns using signal deconvolution techniques. In view of the bandwidth of the piezoelectric elements employed for the detection, the maximum lifetimes detectable by LIOAS are in the order of several μ seconds [13,14].

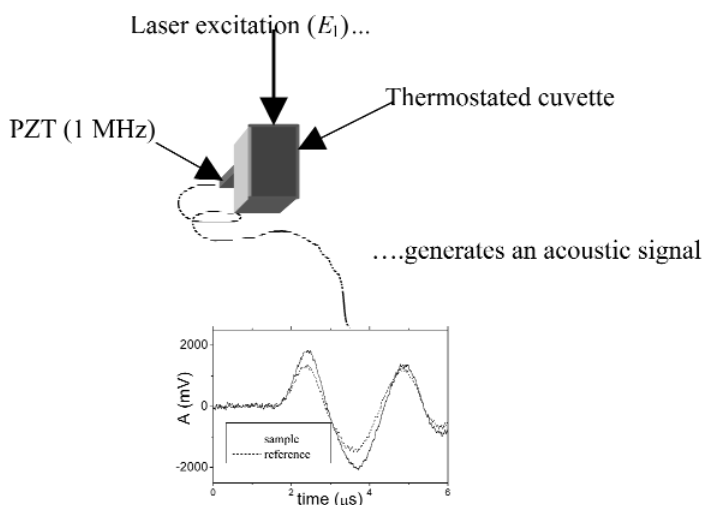


Fig. 1 Schematic representation of an LIOAS experiment.

The LIOAS signals for the sample are a convolution of the equipment response, as determined with a calorimetric reference, and a function representing the time evolution of the pressure upon laser excitation of the sample, often as a sum of single exponential terms (eq. 1). In order to properly assign the various components, the lifetimes (τ_i) are compared to those obtained by other methods, typically transient absorption data from laser flash photolysis.

$$H(t) = \sum_i \frac{\Phi_i}{\tau_i} e^{-\frac{t}{\tau_i}} \quad (1)$$

The amplitudes (Φ_i) are analyzed as a sum of two components, one (α_i) due to heat evolved by radiationless deactivation and the other to changes in volume produced by molecular rearrangements of chromophore and its environment (eq. 2).

$$\Phi_i = \alpha_i + \frac{\Phi_i \Delta V_i}{E_\lambda} \left(\frac{c_p \rho}{\beta} \right); \alpha_i = \frac{q_i}{E_\lambda} \quad (2)$$

Φ_i and ΔV_i are the quantum yield and structural volume change, respectively, associated with the corresponding lifetime τ_i , E_λ is the molar laser energy, c_p , ρ , and β are thermoelastic parameters of the medium (i.e., the heat capacity, the mass density, and the volume expansion coefficient of the medium, respectively), and q_i is the heat evolved during the i^{th} step [12,14].

Several biological energy converters and sensory transducers have been already studied by LIOAS [15]. Other photothermal techniques, such as thermal grating [16] and photothermal beam deflection [17] have been used to resolve shorter-, as well as longer-lived radiationless processes, upon excitation of biological photoreceptors as well as of other photoreactive systems.

LIOAS applied to biological photosensors with isomerizable chromophores

We have unraveled some aspects related to the molecular origin of the time-resolved volume changes for the case of chromoproteins with isomerizable chromophores. Our studies on sensory rhodopsin II from *Natronobacterium pharaonis* have convinced us that there is a compensation between the values of the enthalpy change and the structural volume change associated with the decay lifetime of ca. 1 μ s of the red-absorbing intermediate K to the next intermediate L (ΔH_{KL} and ΔV_{KL}) when measured in various media. This decay is the second component in the LIOAS signal analysis with eq. 1. The first component, associated with K production, has a medium-dependent energy level, but the volume change with respect to the parent compound does not depend on the medium [18].

We interpreted the above-mentioned compensation during K decay as a result of an enthalpy–entropy compensation effect in view of the fact that both thermodynamic quantities (i.e., ΔH_{KL} and ΔV_{KL}) are mainly determined by specific interactions between the chromophore and the medium (the protein environment) by hydrogen bonds and salt bridges. The small changes in environment induce subtle changes in the equilibrium between fluctuating structures (substrates) linked to the various possible chromophore conformations. The value of ΔG_{KL} remains constant because it is intrinsic to the reaction, whereas the values of ΔH_{KL} and ΔS_{KL} depend on the medium and are most probably determined by the strength and number of hydrogen bonds and salt bridges in the different substrates that constitute the ensemble under each specific medium conditions [18].

A negative ΔH vs. ΔS correlation was observed for the formation and decay of K in halorhodopsin from LIOAS measurements of *N. pharaonis* in the presence of various media, but always with Cl^- as the counterion [19]. The ΔH vs. ΔS compensations permitted in the latter cases the calculation of ΔG for the particular reaction under scrutiny. In proteins and in aqueous environments, the values of the structural volume changes could not be explained only by electrostriction (i.e., the solvent reorientation due to changes in dipole moment of the solute). Rather, specific chromophore–protein interactions had

to be invoked to explain the data. The nature of these specific interactions was analyzed by studying model compounds undergoing photoinduced isomerizations (see, e.g., ref. [20]) and ET reactions (vide infra).

ELECTRON-TRANSFER REACTIONS

D1-D2-Cyt b_{559} complexes

The D1-D2-Cyt b_{559} complex isolated from photosystem II (PS II) from green plants and cyanobacteria is the minimum unit able to produce charge separation. According to present knowledge, this complex consists of the D1 and D2 proteins, which bind six chlorophyll (Chl) a , two pheophytin (Pheo) a , and a maximum of two β -carotene molecules (the carotene content depends on the preparation procedure) together with the α - and β -subunits of cytochrome (Cyt) b_{559} [21]. This complex constitutes the core structure of PS II, as can be recognized when analyzing the recent crystallographic structure of PS II from cyanobacteria [22]. In the absence of quinones as secondary electron acceptors, the fate of the photoproduced primary radical pair [P680⁺Pheo⁻] in the D1-D2-Cyt b_{559} complexes is to recombine via radical pair mechanism to the triplet state ³[P680Pheo].

Years ago, we observed an expansion for the formation of ³[P680Pheo] upon pulsed laser excitation at room temperature of D1-D2-Cyt b_{559} complexes from spinach. However, no deconvolution of the signals was carried out during those studies [23]. More recently, in order to understand the role of the β -carotene molecules during excitation and subsequent electron transfer, samples obtained from spinach with various β -carotene contents were studied in our laboratory by LIOAS, employing signal deconvolution techniques. A sum of two single exponential terms ($i = 2$ in eq. 1) described well the time-resolved pressure evolution upon light excitation, i.e., resulted in good fitting of the LIOAS signals. The amplitude of the first exponential term (eq. 2), associated with the production of [P680⁺Pheo⁻] in samples with various β -carotene/chlorophyll ratios and β -carotene in the range of 0.5 to 2 per reaction center, revealed an increase in the structural volume change with increasing β -carotene content (going from a contraction for low β -carotene content to an expansion for large β -carotene content), whereas the energy content and the production quantum yield of [P680⁺Pheo⁻] remained constant for all samples. No influence (within the experimental error) of β -carotene content was observed in the structural volume change associated with the decay of [P680⁺Pheo⁻] to ³[P680Pheo]. From these studies, we concluded that each of the two β -carotene molecules in the D1-D2-Cyt b_{559} complexes plays a different role [24], in agreement with previous observations (see ref. [25]).

Undoubtedly, changes in time-resolved structural volume changes as a function of medium variation reflect subtle changes in chromophore-medium interactions, difficult to observe by other methods.

Electron-transfer studies with model systems

We have studied by LIOAS several inter- and intramolecular ET reactions in aqueous and organic media with the purpose of better understanding the molecular basis of the structural volume changes observed in biological systems.

Various Ru(II)-bipyridyl cyano complexes were analyzed by LIOAS in aqueous solutions at various temperatures. Two exponential terms ($i = 2$ in eq. 1) fitted well the LIOAS signals. The molecular expansion and contraction (ΔV_{str}) for the subnanosecond formation and hundreds of nanoseconds decay, respectively, of the ³MLCT state of [Ru(II)(bpy) _{n} (CN) _{$6-2n$}] ^{$2n-4$} complexes upon photoinduced intramolecular electron transfer were identical, and the magnitude depended on the number of cyano groups in the complex. The ΔV_{str} values were attributed to photoinduced changes in the hydrogen-bond strength between the cyano ligands and the water molecules in the first solvation shell (specific solute-solvent interactions) [26]. Consequently, the linear enthalpy-volume correlation in aqueous salt solutions was interpreted as arising from an enthalpy-entropy compensation effect induced by the

added salt on the hydrogen-bond structure of water. In fact, this was our first observation of an enthalpy- vs.-volume change compensation. This concept was supported by the linear correlation between the ΔV_{str} values in the various salt solutions with the tabulated water-organizing ability of the respective added salt as measured by their standard entropy changes [27].

Clark and Hoffman [28] reported some years ago that the intermolecular ET quenching constant of Ru(II)-tris-bipyridine emission by methyl viologen depended on the anion present. For the same ionic strength of the various monovalent anions employed, the rate of electron transfer was greatest when the dominant anion had the weakest-held hydration sphere and the strongest structure-breaking ability in water, ClO_4^- in their case. Noticeably, the reversible potentials from the cyclic voltammetry experiments for both partners, i.e., for $\text{Ru}(\text{bpy})_3^{3+/2+}$ and for $\text{MV}^{2+/\bullet+}$, were the same in all solutions, irrespective of the nature of the monovalent electrolyte. This obviously means that at identical ionic strength, the free energy for the redox reaction was the same in all electrolytes [28]. These results underline the major role played by the counterion in an ET reaction between partners bearing the same charge sign.

Upon pulsed excitation at 443 nm of $\text{Ru}(\text{bpy})_3^{2+}$ aqueous solutions in the presence of MV^{2+} and the same salts used by Clark and Hoffman, we obtained LIOAS signals that were well fitted by a sum of two exponential terms ($i = 2$ in eq. 1). The preexponential factors associated with each decay (eq. 2) in 0.1 M solutions of various salts were plotted vs. the ratio of thermoelastic parameters for each solution. Examples of the plots are given in Fig. 2. The first term, with a lifetime $\tau_1 < 10$ ns, independent of the counterion present, was assigned to the formation of the $^3\text{MLCT}$ of $\text{Ru}(\text{bpy})_3^{2+}$ (Fig. 2, lower panel). The second term had a lifetime between 100 and 500 ns and a temperature dependence of its amplitude different for the various counterions (Fig. 2, upper panel) [29]. The radical recombination reaction back to the parent system takes place well in the submillisecond time range, exceeding by far the upper limit of the LIOAS experiment (ca. 5 μs). The free-radical ions are the final products in our observation time window.

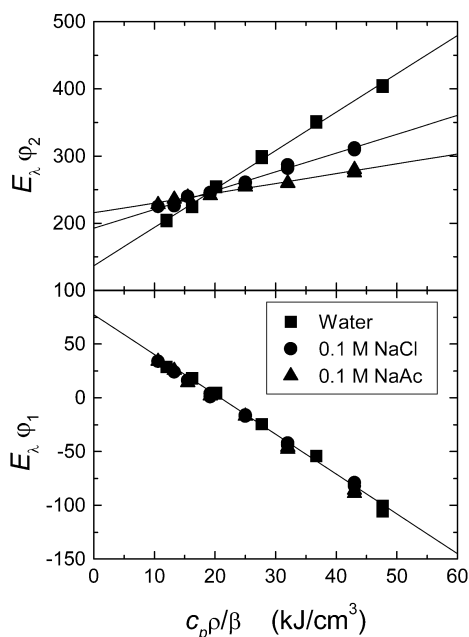


Fig. 2 Amplitudes times molar laser energy vs. the ratio of thermoelastic parameters for the production of $^3\text{MLCT}$ $\text{Ru}(\text{bpy})_3^{2+}$ (lower panel) and its quenching by MV^{2+} yielding the free-radical ions $\text{Ru}(\text{bpy})_3^{3+}$ and $\text{MV}^{\bullet+}$ (upper panel) in the various media as indicated.

After due consideration of the emission by the portion of unquenched ${}^3\text{Ru}(\text{bpy})_3^{2+}$ and the relatively low quantum yield for charge separation in each supporting salt solution, the total redox reaction enthalpy (ΔH_{R}) and the corresponding structural volume changes (ΔV_{R}) linearly correlated with each other (Fig. 3), with an intercept $C = 162 \text{ kJ mol}^{-1}$ coincident with the measured $\Delta G_{\text{R}} = (140 \pm 25) \text{ kJ mol}^{-1}$ [29]. The empirical linear dependence $\Delta H_{\text{R}} = C + X \Delta V_{\text{R}}$ depicted in Fig. 3, together with $C = \Delta G_{\text{R}}$, independent of the supporting salt, and Gibbs equation ($\Delta H_{\text{R}} = \Delta G_{\text{R}} + T\Delta S_{\text{R}}$), leads to the conclusion that the linear $\Delta H_{\text{R}}-\Delta V_{\text{R}}$ correlation is the consequence of an enthalpy–entropy compensation induced by the added salt on the hydrogen-bond network structure of water [29]. Similar considerations were applied later to the $\Delta H_{\text{R}}-\Delta V_{\text{R}}$ compensation found during the studies with the retinal proteins from *Natronobacterium salinarum* (vide supra) [18,19].

Electron-transfer reactions in solution between partners of the same type of charge (i.e., both positive or both negative) should be mediated by the water hydrogen-bond network and the counterions often present in large concentration due to the introduction of buffers. Therefore, in light of the above findings, we reanalyzed the quenching reaction of the xanthene dye erythrosin triplet state (${}^3\text{Er}^{2-}$) by a metal cyanide anion $\text{Mo}(\text{CN})_8^{4-}$, now in the presence of various monovalent cations. This anion was chosen because in our previous work it showed the largest structural volume change among the anions used, albeit a small value in absolute terms [30]. At the concentrations used, the ion-pairing calculations indicate that there is at least a 50 % probability that during the formation of the contact ion pair between ${}^3\text{Er}^{2-}$ and $\text{Mo}(\text{CN})_8^{4-}$, one counterion will be involved during the encounter of the ET partners.

The total quantum yield for the photoproduction of the free radicals $\text{Er}^{3-} + \text{Mo}(\text{CN})_8^{3-}$ upon excitation of Er^{2-} in the presence of $\text{Mo}(\text{CN})_8^{4-}$, as determined by laser flash photolysis by following the transient absorption of the Er^{3-} species at 410 nm, was independent of the counterion present (Li^+ , Na^+ , K^+ , and Cs^+ , all at $4.4 \times 10^{-2} \text{ M}$ analytical concentration) for low reaction conversions. The buffer was in each case the $\text{H}_3\text{BO}_3/\text{B}(\text{OH})_4^-/\text{M}^+$ (pH 9.18 at 20°C).

A sum of two exponentials ($i = 2$ in eq. 1) fitted well the LIOAS signals. Recombination of the separated radicals occurs in the ms time domain with a rate also determined by the counterion, as observed by transient absorbance. Thus, the separated redox free radicals are the final products in the LIOAS time window.

The enthalpy of triplet ${}^3\text{Er}^{2-}$, $\Delta H_1 = (180 \pm 10) \text{ kJ mol}^{-1}$, was obtained from the amplitude (eq. 2) of the first (prompt) term and was independent of the cation. The structural volume change for ${}^3\text{Er}^{2-}$ formation was ΔV_1 ca. 2 mL mol^{-1} , attributed to intrinsic changes upon triplet formation. The pro-

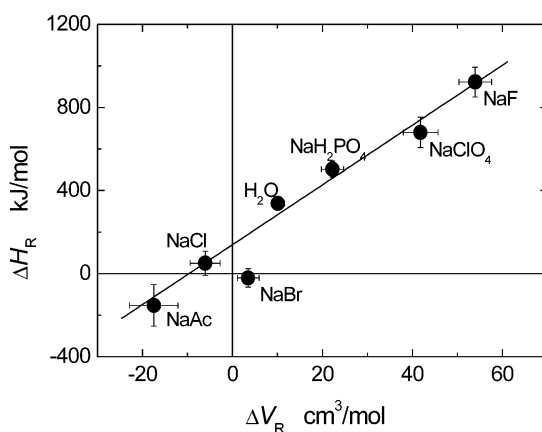


Fig. 3 Structural heat evolved, ΔH_{R} , vs. structural volume change, ΔV_{R} , for the formation of the free-radical ions $\text{Ru}(\text{bpy})_3^{3+}$ and $\text{MV}^{\bullet+}$ from $\text{Ru}(\text{bpy})_3^{2+}$ and 10 mM MV^{2+} in H_2O and in 0.1 M Na^+ salts as indicated ([29] with permission of the American Chemical Society. Copyright owner: American Chemical Society, 1999).

duction of the redox products $\text{Er}^{3-} + \text{Mo}(\text{CN})_8^{3-}$ upon triplet quenching led also to an expansion, ΔV_2 , between 12 mL mol^{-1} for Li^+ and 8 mL mol^{-1} for Cs^+ , which linearly correlated with the heat released during the radical formation step [31].

Also in this case, the correlation was interpreted in terms of an enthalpy–entropy compensation effect, due to the strong influence of the cations on the hydrogen-bond water network, documented by the correlation between ΔV_2 and the literature values for the ability of the cations to organize the water structure [32]. The entropic term for the formation of the free radicals upon triplet quenching assigned to the water network rearrangement was relatively large at room temperature.

The value of ΔV_2 is in principle a sum of electrostrictive and specific effects. The fact that $\Delta V_2 > 0$ can be qualitatively explained by the enlargement of the solvation sphere between the separated radicals, most likely due to an enhanced coulombic repulsion {final: $-3 \times (-3) = 9$ vs. initial: $[-2 \times (-4) = 8]$ }.

The molar volume change due to electrostriction for the reaction from $\text{Er}^{2-} + \text{Mo}(\text{CN})_8^{4-}$ to the free redox products $\text{Er}^{3-} + \text{Mo}(\text{CN})_8^{3-}$ is calculated with Drude–Nernst eq. 3 [33] for each of the ions before and after electron transfer,

$$\Delta V_{\text{el}} = \frac{(ze)^2}{2r\epsilon} \frac{\partial(\ln\epsilon)}{\partial P} = -\frac{Bz^2}{r} \quad (3)$$

where z and r are the charge and the radius of the ion in solution (calculated from crystal data), ϵ is the solvent relative permittivity, and $\partial\ln\epsilon/\partial P$ is its partial derivative with respect to pressure. Should the theoretical value of $B = 4.175 \text{ mL \AA mol}^{-1}$ be used, the values obtained for the oxidation $\text{Mo}(\text{CN})_8^{4-} \rightarrow \text{Mo}(\text{CN})_8^{3-}$ and for the reduction $\text{Er}^{2-} \rightarrow \text{Er}^{3-}$ add up to $\Delta V_{\text{el}} = 5.75 \text{ mL mol}^{-1}$ for the ground-state ET reaction, i.e., less than those derived from the measured values ($\Delta V_{\text{R}} = \Delta V_1 + \Delta V_2$) and certainly independent of the counterion. Using the semiempirical values for B at 25°C between 9.2 and $13.4 \text{ mL \AA mol}^{-1}$ [33], ΔV_{el} between 13 and 18.5 mL mol^{-1} , respectively, are obtained. These values lie closer to those measured for ΔV_{R} , although still independent of the counterion, since the semiempirical B values take into account possible interactions of the solutes with the surrounding water molecules, but not a cationic specific interaction. The cation dependence of the ΔV_2 values indicates a strong component from specific effects during this step. ΔV_2 and ΔH_2 are larger for the case of structure-making Li^+ since the number of hydrogen bonds affected is larger, whereas for the case of structure-breaking Cs^+ , the number of hydrogen bonds involved is smaller.

Factors determining ΔV_{R} in aqueous media; conclusion

The above examples strongly indicate that the values of ΔV_{R} and the associated ΔH_{R} for photoinduced reactions (ET and isomerizations) in aqueous media are mainly determined by specific interactions, such as hydrogen bonds and salt bridges, between the chromophores and the first solvation shell and, in turn, by the structure (e.g., the hydrogen-bond network) of the medium in which the solvated chromophore is embedded. Electrostriction alone is not sufficient to explain the magnitude of the values obtained.

Electron-transfer reactions in organic solvents

The form of eq. 2, readily derived from simple principles [13,14], indicates that it should be possible to separate both contributions to the LIOAS signal amplitude (the enthalpy and the structural volume changes) by varying the ratio $c_p\rho/\beta$.

An alkane series was employed making use of the monotonic change of the ratio $c_p\rho/\beta$ and assuming that ΔH_{R} and ΔV_{R} remain constant along the series [34,35]. The problems derived from this assumption as well as possible new approaches were discussed by Zimmt and Vath [35]. We used slightly different temperatures in the various alkanes such as to keep constant the compressibility, and thus a

constant ΔV_{el} [36]. For some donor-bridge-acceptor (D-B-A) systems undergoing electron transfer upon excitation and showing as a result of the transfer a large transient change in dipole moment, we found that in these nonpolar solvents, electrostriction can explain the time-resolved ΔV_{R} values determined by LIOAS [36,37].

Interestingly, the plots of the time-resolved LIOAS signal amplitudes, following eq. 2 for several photoinduced reactions in a series of alkanes, yield straight lines in spite of the fact that the value of ΔV_{el} calculated with the Drude–Nernst eq. 3 is different for each of the alkanes. Herbrich and Schmidt [38] rationalized this apparent contradiction by noticing that the product $\Delta V_{\text{el}} \times (c_p \rho / \beta)$ is empirically a constant $= \Delta H_{\text{el}}$. Thus, considering that the total structural volume change (as well as the enthalpy change) is a sum of an intrinsic and a solvent-dependent term and that the latter is a result of electrostriction (i.e., $\Delta V_{\text{R}} = \Delta V_{\text{int}} + \Delta V_{\text{solv}} = \Delta V_{\text{int}} + \Delta V_{\text{el}}$), in eq. 2, the constant term $\Delta V_{\text{el}} \times (c_p \rho / \beta)$ becomes part of the intercept. As a consequence, intrinsic enthalpy and structural volume changes (devoid of electrostriction) are derived from the plots with eq. 2. This interesting empirical observation could also be applied to the case of a cycloalkane homologous series used as solvents for the study of the photochemical ring opening of a nitrospiropyrene [20].

However, photochemical reactions, especially ET processes in photosynthetic models, are frequently conducted in polar organic solvents. Thus, we studied the well-known ET reaction between zinc tetraphenylporphine (ZnTPP) and 1,4-benzoquinone (BQ) in a homologous series of nitrile solvents consisting of acetonitrile, propionitrile, butyronitrile, and valeronitrile [39]. The LIOAS signal was again well fitted by a double exponential function ($i = 2$ in eq. 1). The first component, with lifetime τ_1 and amplitude ϕ_1 (eq. 2) was attributed to the triplet $^3\text{ZnTPP}$ formation, whereas τ_2 and ϕ_2 , associated with the second component, were due to the ET quenching of $^3\text{ZnTPP}$ by BQ. In line with previous data for tetrakis-(4-sulfonatophenyl)-porphine in aqueous solution [40], no structural volume change was observed within the experimental error for the formation of $^3\text{ZnTPP}$.

In the nitriles series, the method of variation of $(c_p \rho / \beta)$ cannot be applied, inasmuch as the calculated ΔV_{el} strongly changes along the series (vide supra). Furthermore, $\Delta V_{\text{el}} \times (c_p \rho / \beta)$ is not constant within this series. Thus, the ϕ_2 amplitudes were measured in all four solvents for identical values of τ_2 (i.e., for equal concentration of free ion pairs) and used in eq. 2 together with the measured (by flash photolysis) quantum yields of charge separation Φ_{\pm} . The necessary value of the enthalpy of formation of the ion pair in each solvent was calculated by using eq. 4 [41],

$$E_{\pm} = E_{\text{ox}} - E_{\text{red}} - \frac{Ne^2}{2} \left(\frac{1}{r_{\text{ZnTPP}}} + \frac{1}{r_{\text{BQ}}} \right) \left(\frac{1}{\epsilon_{\text{ace}}} - \frac{1}{\epsilon_{\text{s}}} \right) - \frac{Ne^2}{\epsilon_{\text{s}} r} \quad (4)$$

where E_{ox} and E_{red} are the respective oxidation and reduction potentials of ZnTPP and BQ in acetonitrile, and ϵ_{ace} and ϵ_{s} are the relative permittivities of acetonitrile and the particular solvent. The values of r_{ZnTPP} and r_{BQ} were obtained from literature.

The entropy change of the redox reaction is neglected when using eq. 4 for the calculation of the enthalpy change of charge separation (i.e., $\Delta H_{\pm} = E_{\pm}$) upon $^3\text{ZnTPP}$ quenching by BQ. Thus, the calculated ΔH_{\pm} values should be considered upper limits, because a decrease (albeit probably small) in entropy should be expected upon electron transfer due to the higher order induced by the ions.

By making the energy balance and inserting the calculated E_{\pm} values for the four solvents and the measured Φ_{\pm} values in eq. 2, eq. 5 is obtained, which serves to calculate ΔV_{str} in each solvent

$$\Delta V_{\text{str}} = \left(E_{\pm} - \frac{\Phi_{\text{T}} E_{\text{T}} - \phi_2 E_{\lambda}}{\Phi_{\pm}} \right) \left(\frac{\beta}{c_p \rho} \right)_{\text{s}} \quad (5)$$

Comparison of ΔV_{str} (–12.5, –21.2, –23.6, and –29.5 ml mol^{–1} for acetonitrile, propionitrile, butyronitrile, and valeronitrile, respectively) with the respective ΔV_{el} , calculated with eq. 3 and the data for $(\partial \ln \epsilon / \partial P)_{\text{T}}$ from [32], i.e., $\Delta V_{\text{el}} = -10.9, -13.6, -14.6, \text{ and } -16.6$ ml mol^{–1}, shows that the difference ($\Delta V_{\text{str}} - \Delta V_{\text{el}}$) increases from acetonitrile to valeronitrile having the values –1.6, –7.6, –9.0, and –12.9 ml mol^{–1} for the four solvents. Should the difference be attributed to the entropy change, then the difference would be $(\Delta V_{\text{str}} - \Delta V_{\text{el}}) = -(\beta/c_p \rho) \Delta S$ [42]. In view of the fact that ΔS should be negative (vide supra), $(\Delta V_{\text{str}} - \Delta V_{\text{el}})$ would be positive, in disagreement with the calculated values.

Within the approximations used, a correlation was established between $(\Delta V_{\text{str}} - \Delta V_{\text{el}})$ and Gutman's solvent donor ability [43]. We attributed this correlation to a specific interaction of the free-electron pair of the nitriles aprotic solvents with the ZnTPP⁺ cation [40].

Thus, also in the case of the aprotic nitriles specific solute–solvent interactions should be taken into account, in addition to electrostrictive effects, to explain the values of the structural volume changes upon photoexcitation.

ACKNOWLEDGMENTS

The work reported here is the result of fruitful collaborations with many colleagues, students, and post-doctoral fellows who are coauthors of the cited papers. In particular, I deeply thank Aba Losi for her engagement, ability, and creativity in the projects on biological photoreceptors. I am indebted to Profs. Kurt Schaffner and Wolfgang Lubitz for their support.

REFERENCES

1. J. Heberle. *Biochim. Biophys. Acta* **1458**, 135–147 (2000).
2. A. K. Dioumaev, L. S. Brown, J. Shih, E. N. Spudich, J. L. Spudich, J. K. Lanyi. *Biochemistry* **41**, 5348–5358 (2002).
3. R. P. Sinha and D.-P. Häder. *Photochem. Photobiol. Sci.* **1**, 225–236 (2002).
4. T. P. Sakmar, S. T. Menon, E. P. Marin, E. S. Awad. *Ann. Rev. Biophys. Biomol. Str.* **31**, 443–484 (2002).
5. H. Kandori, Y. Shichida, T. Yoshizawa. *Biochemistry-Moscow* **66**, 1197–1209 (2001).
6. J. Sasaki and J. L. Spudich. *Biochim. Biophys. Acta* **1460**, 230–239 (2000).
7. W. Gärtner and S. E. Braslavsky. In *Photoreceptors and Light Signaling*, A. Batschauer (Ed.), *Comprehensive Series in Photochemical and Photobiological Sciences*, G. Jori and D.-P. Häder (series Eds.), RSC, London (2003). In press.
8. R. D. Viestra and S. J. Davis. *Sem. Cell Develop. Biol.* **11**, 511–521 (2000).
9. T. Lamparter, B. Esteban, J. Hughes. *Eur. J. Biochemistry* **268**, 4720–4730 (2001).
10. T. Gensch, C. C. Gradinaru, I. H. M. van Stokkum, J. Hendriks, K. J. Hellingwerf, R. van Grondelle. *Chem. Phys. Lett.* **356**, 347–354 (2002).
11. W. R. Briggs and J. M. Christie. *Trends Plant Sci.* **7**, 204–210 (2002).
12. J. B. Callis, M. Gouterman, W. W. Parson. *Biochim. Biophys. Acta* **267**, 348–362 (1972).
13. S. E. Braslavsky and G. E. Heibel. *Chem. Rev.* **92**, 13811–1410 (1992).
14. T. Gensch, C. Viappiani, S. E. Braslavsky. In *Encyclopedia of Spectroscopy and Spectrometry*, J. Lindon, G. E. Tranter, J. L. Holmes (Eds.), pp. 1124–1132, Academic Press, New York (1999).
15. P. J. Schulenberg and S. E. Braslavsky. In *Progress in Photothermal and Photoacoustic Science and Technology Vol. III*, A. Mandelis and P. Hess (Eds.), pp. 57–81, SPIE Optical Engineering Press, Washington (1997).
16. Y. Nishioku, M. Nagakawa, M. Tsuda, M. Terazima. *Biophys. J.* **83**, 1136–1146 (2002).
17. I. Michler and S. E. Braslavsky. *Photochem. Photobiol.* **74**, 624–635 (2001).

18. A. Losi, A. A. Wegener, M. Engelhard, S. E. Braslavsky. *J. Am. Chem. Soc.* **123**, 1766–1767 (2001).
19. A. Losi, A. A. Wegener, M. Engelhard, S. E. Braslavsky. *Photochem. Photobiol.* **74**, 495–503 (2001).
20. R. M. Williams, G. Klihm, S. E. Braslavsky. *Helv. Chim. Acta* **84**, 2557–2576 (2001).
21. L. Konermann and A. R. Holzwarth. *Biochemistry* **35**, 829–842 (1996).
22. A. Zouni, H. T. Witt, J. Kern, P. Fromme, N. Krauss, W. Sanger, P. Orth. *Nature* **409**, 739–743 (2001).
23. I. Yruela, M. S. Churio, T. Gensch, S. E. Braslavsky, A. R. Holzwarth. *J. Phys. Chem.* **98**, 12789–12795 (1994).
24. A. Losi, I. Yruela, M. Reuss, S. E. Braslavsky, A. R. Holzwarth. *Photochem. Photobiol. Sci.* **2** (2003); published on the Web 3 June 2003, DOI 10.1039/b301282d.
25. C. A. Tracewell, J. C. Vrettos, J. A. Bautista, H. A. Frank, G. W. Brudvig. *Arch Biochem. Biophys.* **385**, 61–69 (2001).
26. J. L. Habib-Jiwan, B. Wegewijs, M. T. Indelli, F. Scandola, S. E. Braslavsky. *Recl. Trav. Chim. Pays-Bas* **114**, 542–548 (1995).
27. C. D. Borsarelli and S. E. Braslavsky. *J. Phys. Chem. B* **102**, 6231–6238 (1998).
28. C. D. Clark and M. Z. Hofmann. *J. Phys. Chem.* **100**, 7526–7532 (1996).
29. C. D. Borsarelli and S. E. Braslavsky. *J. Phys. Chem. A* **102**, 1719–1727 (1999).
30. J. L. Habib-Jiwan, A. K. Chibisov, S. E. Braslavsky. *J. Phys. Chem.* **99**, 10246–10250 (1995).
31. E. Yeow, L. D. Slep, A. K. Chibisov, S. E. Braslavsky. *J. Phys. Chem. A* **107**, 439–446 (2003); Correction: *ibid*, 2118.
32. Y. Marcus. *Ion Solvation*. Wiley, New York (1985).
33. F. J. Millero. *Chem. Rev.* **71**, 147–176 (1971).
34. R. R. Hung and J. J. Grabowski. *J. Am. Chem. Soc.* **114**, 351–353 (1992).
35. M. B. Zimmt and P. A. Vath. *Photochem. Photobiol.* **65**, 10–14 (1997).
36. B. Wegewijs, M. N. Paddon-Row, S. E. Braslavsky. *J. Phys. Chem. A* **102**, 8812–8818 (1998).
37. B. Wegewijs, J. W. Verhoeven, S. E. Braslavsky. *J. Phys. Chem.* **100**, 8890–8894 (1996).
38. R. P. Herbrich and R. Schmidt. *J. Photochem. Photobiol. A: Chemistry* **133**, 149–158 (2000).
39. E. K. L. Yeow and S. E. Braslavsky. *Phys. Chem. Chem. Phys.* **4**, 239–247 (2002).
40. T. Gensch, C. Viappiani, S. E. Braslavsky. *J. Am. Chem. Soc.* **121**, 10573–10582 (1999).
41. G. J. Kavarnos. *Fundamentals of Photoinduced Electron Transfer*, VCH, New York (1993).
42. D. Mauzerall, J. Feitelson, R. Prince. *J. Phys. Chem.* **99**, 1090–1093 (1995).
43. C. Reichardt. *Solvent Effects in Organic Chemistry*, Verlag Chemie, Weinheim (1979).